Hydration Force and Bilayer Deformation: A Reevaluation†

T. J. McIntosh*
Department of Anatomy, Duke University Medical Center, Durham, North Carolina 27710
S. A. Simon
Departments of Physiology and Anesthesiology, Duke University Medical Center, Durham, North Carolina 27710
Received October 11, 1985; Revised Manuscript Received March 12, 1986

ABSTRACT: The hydration repulsive force between lipid bilayers and the deformability of both gel and liquid-crystalline bilayers have been quantitated by an X-ray diffraction analysis of osmotically stressed liposomes. Both sampling theorem reconstructions and electron density distributions were calculated from diffraction data obtained from multilayers with applied osmotic pressures of 0–50 atm. The bilayer thickness and area per lipid molecule remain nearly constant (to within about 4%) in this pressure range, as adjacent bilayers move from their equilibrium separation in excess water to within 2–4 Å of each other. This analysis indicates that the bilayers are relatively incompressible. This result differs from previously published X-ray diffraction studies of bilayer compressibility but agrees with direct mechanical measurements of the bilayer compressibility modulus. It is also found that the hydration repulsive force decays exponentially with separation between bilayers with a decay constant of 1.4 Å for gel-state dipalmitoylphosphatidylcholine and 1.7 Å for liquid-crystalline egg phosphatidylcholine bilayers. This implies that the exponential decay constant is not necessarily equal to the diameter of a water molecule, as has been previously suggested on experimental and theoretical grounds.

The main barrier to adhesion of two polar or charged surfaces in solution is the hydration repulsive force, F_h (LeNeveu et al., 1976; Pashley, 1983; Israelachvili & Pashley, 1983). This short-range force is therefore important in studies of coagulation of colloids (Derjaguin & Chureav, 1977), swelling of clays (van Olphen, 1977), thinning of soap films (Clunie et al., 1967), aggregation of gas bubbles (Melville & Matijevic, 1976), interactions of macromolecules such as DNA (Rau et al., 1984), and fusion of lipid vesicles and biological membranes (Parsegian & Rand, 1983; Horn, 1984).

For membranes and lipid bilayers, F_h has been determined quantitatively in the pioneering work of Rand, Parsegian, and colleagues (LeNeveu et al., 1976, 1977; Parsegian et al., 1979; Rand et al., 1981; Lis et al., 1981, 1982a,b). They have shown for a variety of lipid bilayer systems that F_h decays exponentially as a function of fluid layer thickness, d_f, so that $F_h = F_0 \exp(-d_f/\lambda)$, where λ is the decay constant. To obtain the dependence of F_h on d_f, these investigators (LeNeveu et al., 1976, 1977) have developed an elegant "osmotic stress" method, whereby osmotic pressures are applied to lipid bilayers by incubating liposomes in solutions of high molecular weight neutral polymers, such as poly(vinylpyrrolidone) (PVP)[1] or dextran. Since these polymers are too large to enter between the multilayers, they compete for water with the lamellar lattice and therefore compress it (LeNeveu et al., 1977). For each liposome–polymer suspension, X-ray diffraction provides the lamellar repeat period (d), which is the sum of the bilayer thickness (d_b) and d_f. The most difficult part of the analysis is to separate d_f from d. Rand, Parsegian, and colleagues (LeNeveu et al., 1977; Parsegian et al., 1979; Lis et al., 1982) have calculated d_f by a two-step procedure whereby a relationship between d_f and d was obtained from a separate set of lipid–water mixtures and then used to set d_f for each value of d measured in the osmotic stress experiments. For each lipid–water mixture, d_f and d_b were set equal to the partial thickness (Luzzati, 1968; Tardieu et al., 1973) of water and lipid, respectively, and were calculated from d and the gravimetrically determined volume fraction of lipid (ϕ_L) under the assumption that the partial specific volumes of water and lipid are equal to 1.0 over the entire range of hydration. For each lipid–water mixture, the area per lipid molecule, A_l, was also calculated from d_b by use of the formalism of Luzzati (1968). Three of the important conclusions from this and other published work are as follows: (1) the bilayer thickness is significantly changed by the close approach of the adjacent bilayer (Small, 1967; LeNeveu et al., 1976, 1977; Parsegian et al., 1979; Lis et al., 1981); (2) lateral compression can cause large area changes (Parsegian & Rand, 1983; LeNeveu et al., 1977; Lis et al., 1982a,b); and (3) the exponential decay constant, λ, has the approximate dimensions of a water molecule (Lis et al., 1982a; Schiby & Ruckenstein, 1983; Cevc & Marsh, 1985).

In this paper, we reevaluate these three conclusions by applying Fourier synthesis methods to X-ray diffraction data from both gel and liquid-crystalline bilayers. We use the same osmotic stress method (LeNeveu et al., 1976,1977; Lis et al., 1981; Rand, 1981), except that we do not use partial lipid and water thicknesses for d_b and d_f, respectively, but instead use dimensions obtained from electron density profiles of each lipid–polymer system. Thus, measurements of water contents of separate lipid–water specimens are avoided. Using the Fourier approach, we find that the bilayer thickness and area remain nearly constant as adjacent bilayers approach each other. In agreement with previous work (LeNeveu et al., 1977; Parsegian et al., 1979; Lis et al., 1982a), we find that the hydration force decays exponentially as a function of fluid layer

† This research was supported by a grant from the National Institutes of Health (GM-27278) and a gift from the R. J. Reynolds Corp.

[1] Abbreviations: DPPC, dipalmitoylphosphatidylcholine; EPC, egg phosphatidylcholine; BPE, bacterial phosphatidylethanolamine; DMPC, dimyristoylphosphatidylcholine; PC, phosphatidylcholine; PE, phosphatidylethanolamine; PVP, poly(vinylpyrrolidone).

0006-2960/86/0425-4058$01.50/0

Table I: Structure Amplitudes

polymer	ln P (dyn/cm^2)	d (Å)	$F(1)$	$F(2)$	$F(3)$	$F(4)$	$F(5)$
			DPPC				
0% PVP		63.6	5.37	4.49	2.65	2.03	1.72
10% PVP	12.97	63.2	5.55	4.11	2.50	2.62	1.53
20% PVP	14.64	61.7	4.97	4.28	2.76	3.22	
30% PVP	15.75	60.5	5.39	4.02	2.34	3.13	
40% PVP	16.59	59.7	5.24	4.13	2.15	3.25	
50% PVP	17.27	58.7	5.16	3.30	2.28	4.00	
60% PVP	17.86	57.8	6.14	2.32	1.50	3.53	
5% dextran	10.72	63.4	5.03	4.88	2.50	2.02	1.97
25% dextran	14.73	62.3	5.42	4.40	2.67	2.22	1.21
30% dextran	15.27	61.6	5.20	4.07	2.67	2.91	1.56
35% dextran	15.75	61.2	6.31	3.15	2.23	2.38	0.91
20% dextran[a]	14.09	62.6					
			EPC				
0% PVP		63.2	5.06	5.31	2.44	0	1.85
10% PVP	12.97	59.2	5.38	4.68	2.41	0	1.60
20% PVP	14.64	56.0	5.36	4.08	2.80	1.05	1.22
30% PVP	15.75	54.5	5.48	3.61	2.95	1.66	
40% PVP	16.59	53.0	5.66	3.17	2.99	1.53	
50% PVP	17.27	52.4	5.92	2.38	2.65	2.16	
60% PVP	17.86	51.7	6.26	1.55	2.18	2.31	
30% dextran	15.27	55.2	5.53	3.52	3.19	1.42	
40% dextran	16.17	54.6	5.56	3.37	2.88	2.00	
50% dextran	16.92	52.4	5.35	3.14	3.10	2.07	
20% dextran[a]	14.09	58.5					
			BPE				
0% PVP		53.4	6.10	0.98	1.82	3.46	
10% PVP	12.97	52.6	6.50	0.81	1.45	2.75	
20% PVP	14.64	51.9	6.58	0.39	1.17	2.64	
30% PVP	15.75	51.3	6.68	0	0.93	2.40	
45% PVP	16.95	50.5	6.46	0.27	0	2.97	
60% PVP	17.86	49.9	6.68	0.88	0	2.16	

[a] Diffraction patterns for these specimens were recorded on a long camera, and only 2 orders of diffraction were observed.

thickness. However, our values for the decay constant, λ, are somewhat smaller than both the previously reported values and the diameter of a water molecule. Our results are consistent with the recent force measurements of Marra and Israelachvili (1985) and consistent with the compressibility moduli measured directly for unilamellar vesicles (Kwok & Evans, 1981; Evans & Kwok, 1982).

Materials and Methods

Dipalmitoylphosphatidylcholine (DPPC), egg phosphatidylcholine (EPC), and bacterial phosphatidylethanolamine (BPE) were used as obtained from Avanti Biochemicals. Lipid purity was periodically checked by thin-layer chromatography with a developing solvent of $CHCl_3$–MeOH–NH_4OH (65:25:5 by volume). A single spot was always observed for each sample tested (100 μg of lipid). Dextran (average molecular weight 255 000, lot number 776-0336) and poly(vinylpyrrolidone) (average molecular weight 40 000, lot number 45F-0372) were obtained from Sigma Chemical Co. Triply distilled water was used to make dextran–water solutions in the range of 0–50% w/w and PVP–water solutions in the range of 0–60% w/w. For the dextran and PVP solutions, we used values of osmotic pressure as calculated from the virial coefficients of Vink (1971). These pressures for dextran are in close agreement with the measured values of LeNeveu et al. (1977).

Lipid–polymer suspensions were formed by incubating the lipid in excess amounts (greater than 70%) of the appropriate polymer solution and allowing the suspension to incubate several hours at temperatures above the lipid phase transition temperature. In these specimens, the excess phase was always visible either by direct observation or by light microscopy.

For X-ray diffraction experiments, the suspensions were sealed in quartz glass capillary tubes and mounted in a pinhole collimation X-ray camera containing three or more sheets of Kodak DEF-5 X-ray film in a flat plate film cassette. Specimen to film distance was 10 cm, and exposure times were on the order of 3–12 h. The films were processed by standard techniques and densitometered with a Joyce-Loebl Model MKIIIC microdensitometer. The background curve was subtracted, and integrated intensities, $I(h)$, for each diffraction order (h) were obtained by measuring the area under each diffraction peak. For these unoriented suspensions, the structure amplitude for order h was set equal to $[h^2I(h)]^{1/2}$. For each lipid series, structure amplitudes were normalized according to the procedure of Blaurock (1971). Phase angles were assigned as described under Results, and electron density profiles were calculated as described previously (McIntosh, 1980). Continuous transforms were calculated by use of the sampling theorem (Shannon, 1949) as described by McIntosh et al. (1983).

For certain specimens (see Table I), diffraction patterns were recorded by using a double-mirror camera and a longer (21 cm) specimen to film distance. For these specimens, only the first two orders of the lamellar diffraction were recorded.

Results

For all lipids analyzed, diffraction patterns consisted of orders of a lamellar repeat period and one or two wide-angle bands. Table I presents structure amplitudes and repeat periods for phosphatidylcholine and phosphatidylethanolamine bilayers for a series of osmotic pressure experiments. The structure amplitudes for gel-state ($L_{\beta'}$) DPPC and liquid-crystalline (L_α) EPC are presented in panels A and B, respectively, of Figure 1 as a function of the reciprocal space coordinate. For DPPC, d ranges from 63.6 Å in water to 57.8 Å in 60% PVP, while for EPC, d ranges from 63.2 Å in water

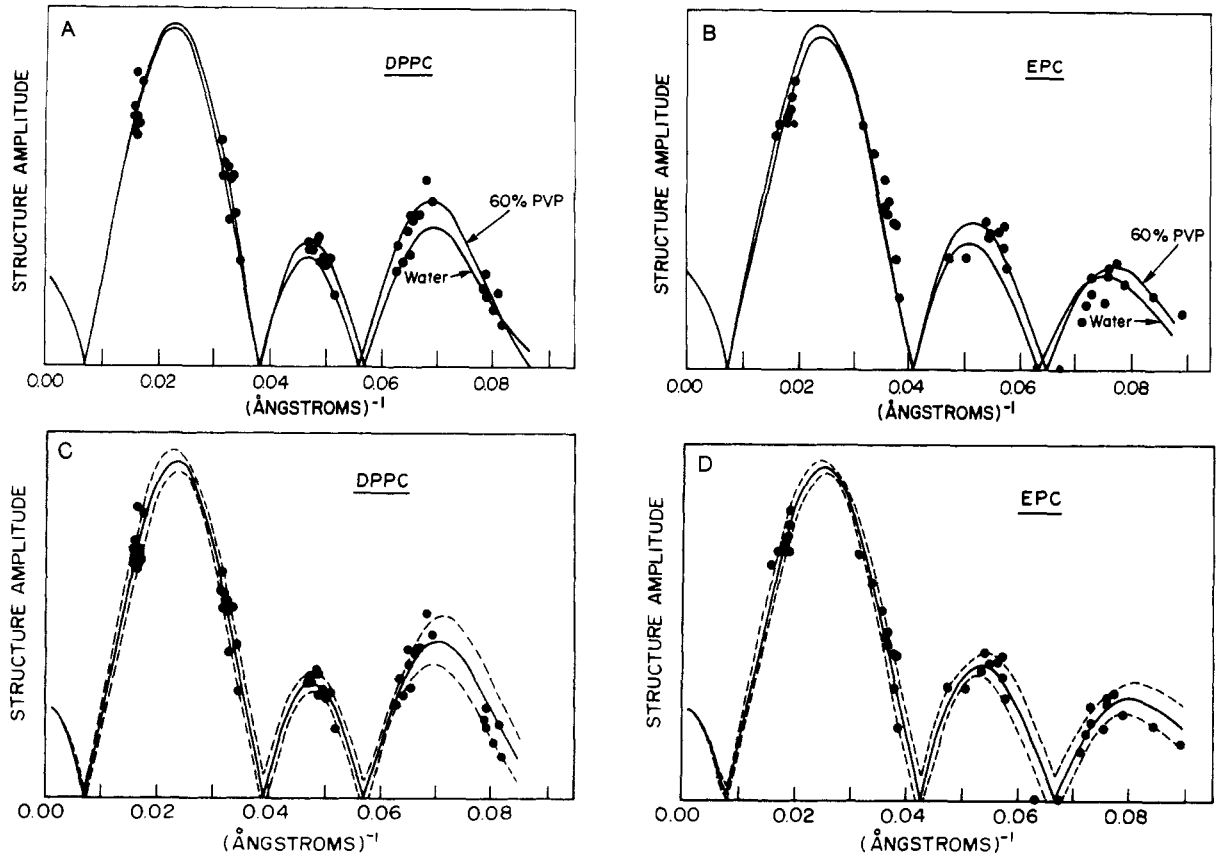

FIGURE 1: Structure amplitudes for DPPC (A and C) and EPC (B and D). The circles represent observed structure amplitudes for osmotic pressure experiments in PVP (0–60 wt %) and dextran (0–50 wt %) solutions. In (A) and (B), the solid curves are absolute values of sampling theorem reconstructions of the continuous transform using data from lipid in water and in 60% PVP, which represent the extreme values of repeat period found in these experiments. In (C) and (D), the solid curves are mean values of all transforms calculated with the data in Table I, and the dashed curves show ± one standard deviation from the mean.

to 51.7 Å in 60% PVP. The pairs of solid curves in Figure 1A,B are absolute values of continuous transforms calculated by application of Shannon's sampling theorem (Shannon, 1949) to the structure factor data for these extreme repeat periods using the phase combinations previously determined (Lesslauer et al., 1972; Torbet & Wilkins, 1976). The value of the structure amplitude at the origin was determined by the method of King and Worthington (1971). For both DPPC and EPC, these pairs of transforms superimpose quite closely in that the nodes and maxima occur at nearly the same positions in reciprocal space. This indicates that the thickness of the bilayer is nearly constant over this range of d (Worthington et al., 1973). These transforms are quite similar to previously published transforms of these lipids (Torbet & Wilkins, 1976).

To better visualize the experimental uncertainty in these measurements, we have calculated, point by point, the mean transform and the standard deviation for all data sets for DPPC (N = 11 experiments) and EPC (N = 10 experiments). These mean transforms are shown with solid lines in Figure 1C,D, with the standard deviations displayed as dashed lines.

Figure 2 shows electron density profiles calculated for DPPC and EPC in water and in 60% PVP. For each profile, the origin is located at the center of one bilayer, and one unit cell is shown. Each unit cell contains two half-bilayers plus the fluid space between bilayers. As illustrated by the schematic drawings at the top of Figure 2A,B, the low-density troughs centered at the origin correspond to the localization of the lipid terminal methyl groups, the adjacent medium-density plateaus correspond to the methylene chain regions, and the highest density peaks centered at 21 Å for DPPC and 19 Å for EPC correspond to the lipid polar head groups. Immediately outside each head group peak is another medium-density region which corresponds to the fluid space between bilayers. The head-group peak of the adjacent bilayer is seen on the other side of each fluid space. For both DPPC and EPC, the profiles superimpose quite closely from the origin (at the bilayer center) to the edge of the bilayer, indicating that the bilayer structure is similar in water and in 60% PVP. These profiles also show that the fluid space between bilayers is reduced by incubating the liposomes in 60% PVP, as the head-group peaks of adjacent bilayers are significantly closer in the presence of 60% PVP (Figure 2A,B). Electron density profiles from a series of osmotic stress experiments are shown in panels A and B of Figure 3 for DPPC and EPC, respectively. These profiles indicate (1) that the fluid space between adjacent bilayers decreases monotonically as the concentration of PVP increases and (2) that the bilayer thickness remains approximately constant for this range of PVP concentrations. The distance between head-group peaks across the bilayer for the experiments listed in Table I is 41.9 ± 0.6 Å (mean ± SD; N = 11 experiments) for DPPC and 37.8 ± 0.8 Å (N = 10) for EPC.

To quantify the decrease in fluid space produced by the different PVP and dextran solutions, we have used dimensions obtained from the electron density profiles shown in Figure 3 and from similar profiles (not shown) obtained from dextran solutions. Lesslauer et al. (1972) have shown that, at this resolution, the high-density peaks in the profile fall near the center of the phosphatidylcholine head group, between the phosphate moiety and the glycerol backbone. Space-filling molecular models show that the distance from the center to the outer edge of the PC head group is approximately 5 Å.

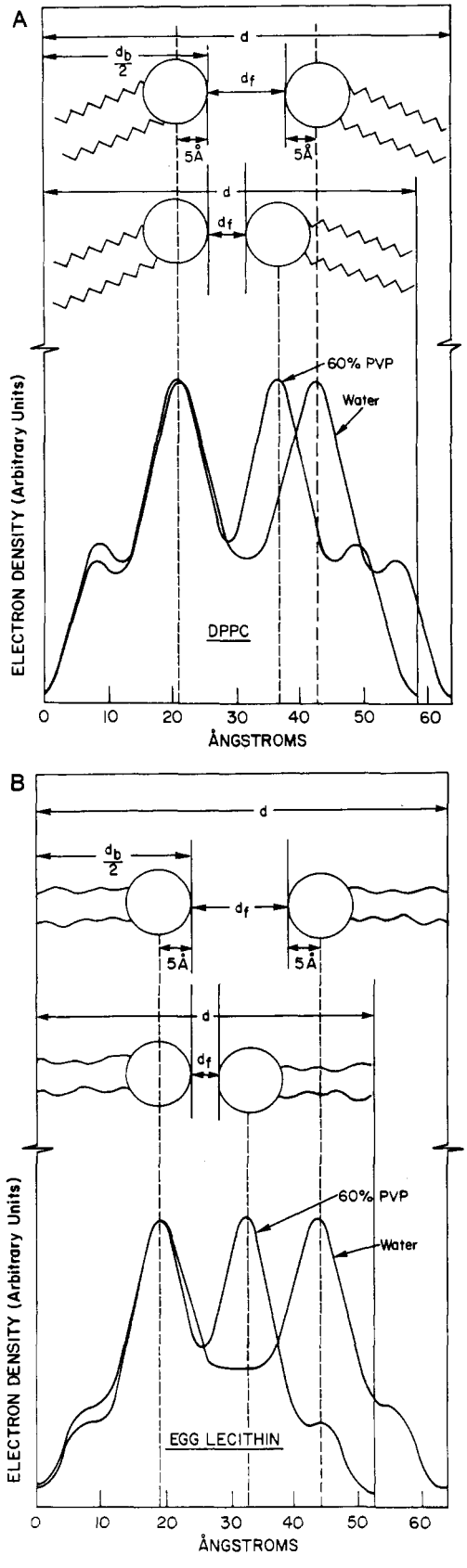

FIGURE 2: Electron density profiles for DPPC (A) and EPC (B) in excess water and in 60% PVP. In each profile, the origin is located at the center of the bilayer, and one unit cell is shown. Schematic drawings of the lipid molecules are shown above the profiles, with circles representing the lipid head groups, jagged lines representing gel-state hydrocarbon chains, and wavy lines representing liquid-crystalline hydrocarbon chains. In DPPC, the hydrocarbon chains are tilted relative to the normal to the plane of the bilayer (Tardieu et al., 1973).

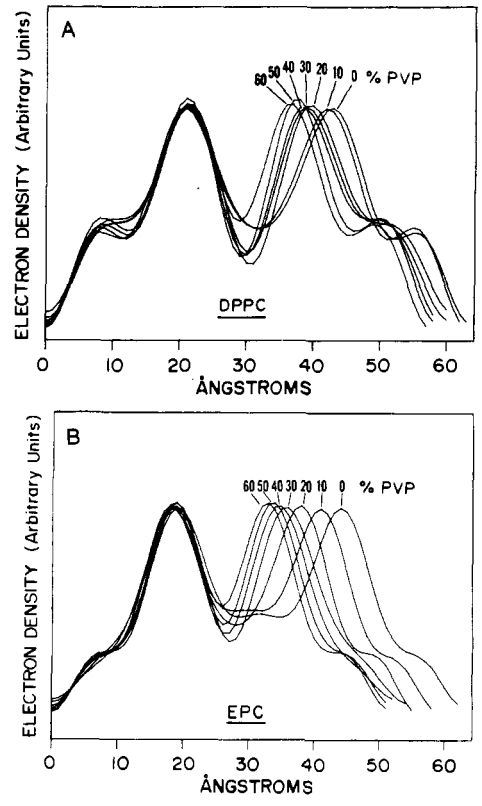

FIGURE 3: Electron density profiles calculated for DPPC (A) and EPC (B) in water and 10%, 20%, 30%, 40%, 50%, and 60% PVP solutions. The origin is located at the center of the bilayer for each profile. The profiles were put on the same scale by normalizing the structure factors according to the procedure of Blaurock (1971).

Therefore, for PC bilayers, we define d_b as the distance between high-density peaks across the bilayer plus 10 Å. Thus, d_b = 51.9 Å for DPPC and 47.8 Å for EPC. The fluid layer thickness is calculated by $d_f = d - d_b$ (see schematic diagrams at top of Figure 2A,B) and is 11.7 Å for DPPC and 15.4 Å for EPC in water.

Figure 4A shows structure amplitudes for an osmotic stress series with a liquid-crystalline lipid having a different polar head group, bacterial phosphatidylethanolamine (BPE). The range of repeat periods in this series is 53.4 Å in water to 49.9 Å in 60% PVP. The two solid curves are continuous transforms calculated with structure factors for BPE in water and in 60% PVP solution using equivalent phase angles to those used by Simon et al. (1982). Clearly, the two continuous transforms superimpose quite closely. Especially significant is the observation that the nodes and peaks of the two transforms occur at the same positions in reciprocal space. This is excellent evidence that the bilayer thickness is, within experimental uncertainty, the same for BPE in water or in 60% PVP. The mean transform ± the standard deviation for the six data sets (Table I) is shown in Figure 4B. Electron density profiles for PBE in 0, 30, and 60% PVP solutions are shown in Figure 4C. As was the case for PC bilayers (Figures 2 and 3), these profiles in Figure 4C show that increasing PVP concentrations force the BPE bilayers closer together, without changing the bilayer thickness. The distance between headgroup peaks across the bilayers for the BPE experiments listed in Table I is 39.6 ± 0.4 Å (N = 6). At 60% PVP, the BPE bilayers are close enough together that the electron density of the fluid space is elevated due to the overlap of the headgroup density peaks. To estimate d_b and d_f from the electron density profiles (Figure 4C), we use the analysis of Hitchcock et al. (1974), who found in electron density profiles at this

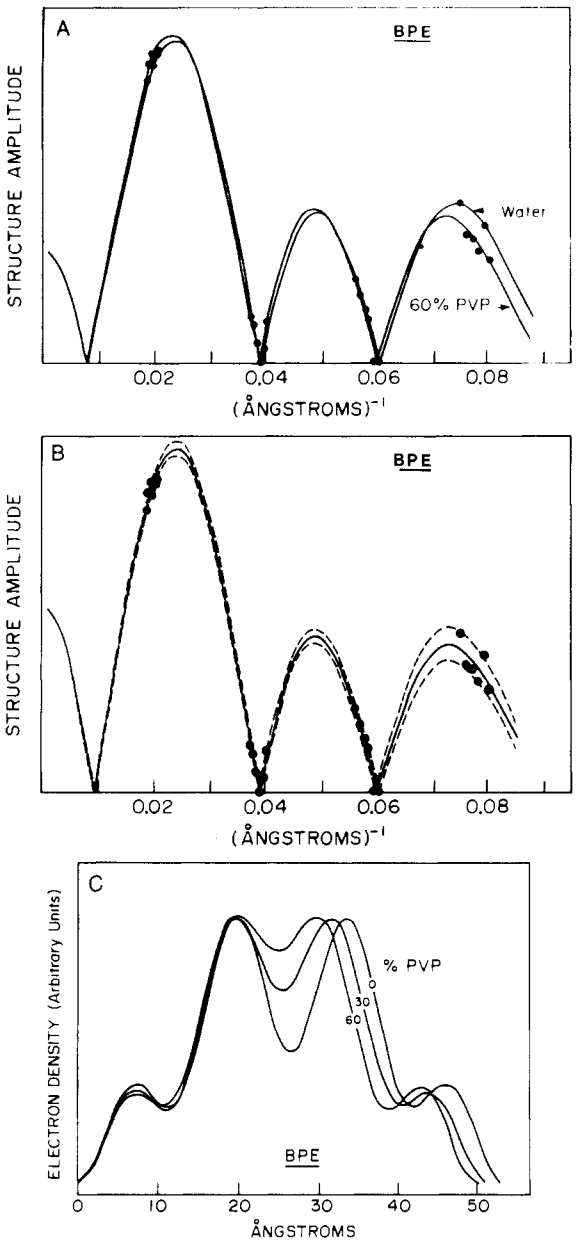

FIGURE 4: Structure amplitudes (A and B) and electron density profiles (C) for BPE bilayers in water and PVP solutions. In (A), the circles represent experimental structure factors, and the solid lines are absolute values of sampling theorem reconstructions of the continuous transforms for BPE in water and in 60% PVP. In (B), the solid curve is the mean value of all transforms calculated with the data in Table I, and the dashed curves show one standard deviation from the mean. In (C), the origin is located at the center of the bilayer for each profile.

resolution that the head-group peak for dilauroyl-PE is located between the phosphate moiety and the glycerol backbone of the lipids. Space-filling molecular models show that the PE head group is smaller than the PC head group and that the distance between the center and outer edge of the PE head group is approximately 4 Å. Therefore, for BPE bilayers, we define d_b as the distance between high-density head-group peaks across the bilayer plus 8 Å. Using this definition of d_b and the electron density profiles for BPE, we find that the bilayer thickness is 47.6 Å and d_f decreases from 5.8 Å in excess water to 2.3 Å in 60% PVP. These fluid spaces are quite small, especially considering that the diameter of a water molecule is about 2.8 Å. Thus, one obvious difference between PC and PE bilayers is the width of the fluid space between bilayers. In water, the d_f is about 10 Å smaller for BPE as compared to EPC. This observation is similar to the results of LeNeveu et al. (1977) and Lis et al. (1982a), who found that the partial fluid thickness is smaller for egg PE than EPC in water. It should be noted, however, that Lis et al. (1982a) found a partial fluid thickness of 20.5 Å for egg PE in water, which is significantly larger than the fluid space observed in electron density profiles of BPE in water (Figure 4C). Marra and Israelachvili (1985) also found that the equilibrium spacings are about 10 Å smaller for gel-state PE's compared to gel-state PC's.

Thus, comparisons of both the continuous transforms (Figures 1A,B and 4A) and the electron density profiles (Figures 2A,B, 3A,B, and 4C) indicate that, at this resolution, the bilayer thickness for DPPC, EPC, and BPE remains nearly constant as the adjacent bilayers move from their equilibrium separation to within 2–4 Å of each other. One potential difficulty with this type of comparison is the limited resolution of the X-ray data, to about 1/12 Å in reciprocal space. However, since we are measuring changes in the positions of two widely spaced and well-defined peaks, namely, the head-group peaks in the electron density profiles, this resolution is sufficient to detect changes in bilayer thickness greater than 1–2 Å. The following model calculations illustrate the sensitivity of the method and show that relatively small changes in bilayer thickness would produce detectable changes in both the continuous transforms and the electron density profiles. Absolute values of continuous transforms of four electron density strip model bilayers with bilayer thicknesses of 48, 50, 52, and 54 Å are shown in Figure 5A. Note that in these model calculations the nodes and maxima in the transforms systematically move to smaller values of reciprocal space as the bilayer thickness increases. No such systematic movement of nodes or maxima is observed in the transforms generated from the experimental data (Table I) with increasing polymer concentration. Comparisons of the model transforms (Figure 5A) with the experimental transforms shown in Figures 1C,D, and 4B indicate that the experimental uncertainty for DPPC and BPE is smaller than the change in transform caused by a 1-Å change in bilayer thickness and that the experimental uncertainty for EPC is smaller than a 2-Å change in bilayer thickness. We note that approximately a 6-Å change in partial lipid thickness was found by Parsegian et al. (1979) and Lis et al. (1982a) for EPC and DPPC, respectively, for the range of repeat periods presented in this paper. Electron density profiles of two strip models differing by 6 Å in thickness are shown in Figure 5B. This 6-Å change in thickness produces a much larger change in head-group peak separation across the bilayer in these profiles (Figure 5B) than is observed in the experimental profiles (Figures 2A,B and 3A,B).

Another important piece of evidence concerning changes in bilayer structure is the wide-angle diffraction pattern of the gel-state lipid. For DPPC in excess water, the hydrocarbon chains are packed in a "quasi-hexagonal" array with the chains inclined or tilted relative to the normal to the plane of the bilayer (Tardieu et al., 1973). As shown by Tardieu et al. (1973), this packing gives rise to a characteristic double wide-angle reflection. For the bilayer to change in thickness, either the distance between chains or the chain tilt must change. However, we find that, within experimental uncertainty (±0.02 Å), the spacings and widths of these wide-angle reflections are the same for DPPC in water or in the PVP and dextran solutions used in these experiments. That is, the wide-angle pattern contains a sharp reflection at 4.20 Å and a broad band centered at 4.09 Å over the entire range of osmotic pressures, from 0% to 60% PVP. Thus, within ex-

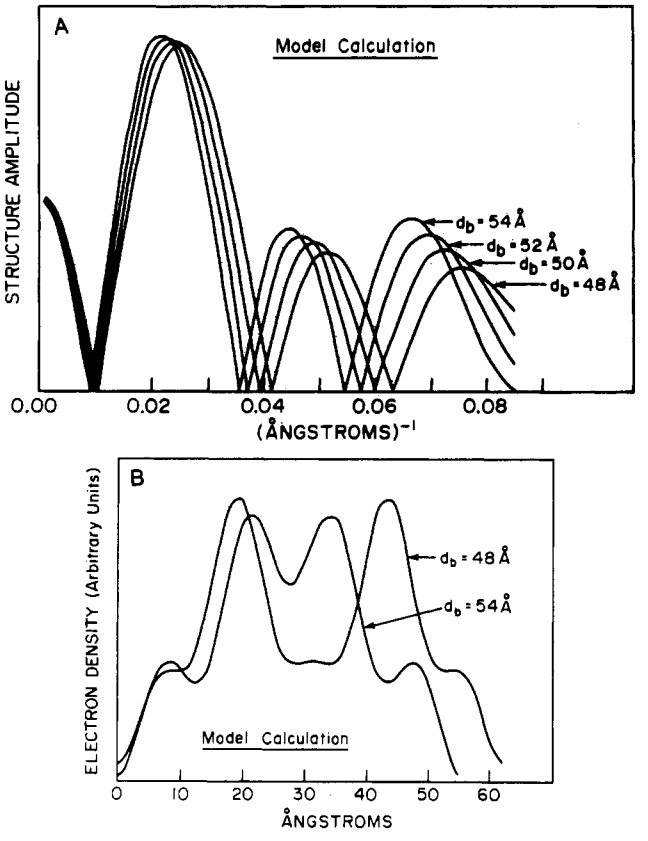

FIGURE 5: Continuous transforms (A) of four bilayer strip models with bilayer thickness, d_b, of 48, 50, 52, and 54 Å, and electron density profiles (B) of bilayer strip models with bilayer thicknesses of 48 and 54 Å. All models have five uniform-density strips corresponding to the terminal methyl region, two methylene chain regions, and two head-group regions, with electron densities of 0.25, 0.32, and 0.44 e/Å^3, respectively, which are similar to published bilayer models (King, 1984; Franks et al., 1982). For d_b = 48 Å, the widths are 7, 10.5, and 10 Å for the terminal methyl, methylene chain, and head-group regions, respectively. For d_b = 50, 52, and 54 Å, the widths of the methylene chain regions are 11.5, 12.5, and 13.5 Å, respectively, with the widths of the terminal methyl and head-group regions unchanged. In this model calculation, we assume that the volume of the bilayer is constant for this range of repeat periods. For the electron density profiles of (B), repeat periods of 63 and 56 Å were chosen for d_b = 48 Å and d_b = 54 Å, respectively.

perimental uncertainty, the chain to chain separation and chain tilt—and hence the area per lipid molecule—do not change under these conditions. Levine (1970) has also found, by direct observation of the position of the wide-angle reflection from oriented specimens, that the chain tilt does not change from full hydration down to 15% water content.

Figure 6 compares plots of the natural logarithm of osmotic pressure vs. d_f for DPPC and EPC using the values of d_f obtained from measurements of ϕ_L by Lis et al. (1982a) (dashed lines) and by our Fourier synthesis approach (solid lines). Except for values of d_f within 1–3 Å of the equilibrium separation, the data points fall on straight lines, indicating that F_h decays exponentially with d_f as previously found (LeNeveu et al., 1977; Parsegian et al., 1979; Lis et al., 1981, 1982a). From the slopes of these solid lines, we obtain decay constants for F_h of 1.35 Å for DPPC and 1.71 Å for EPC, which can be compared to the published values of 2.1 Å for DPPC (Lis et al., 1982a) and 1.9 Å (LeNeveu et al., 1977) or 2.6 Å for EPC (Parsegian et al., 1979; Lis et al., 1982a) and 5–7.5 Å for bilayers made from surfactants deposited on mica plates (Pashley & Israelachvili, 1981).

The osmotic pressure axis intercept of the curves in Figure 6 is related to the contact energy (E_c) between bilayers

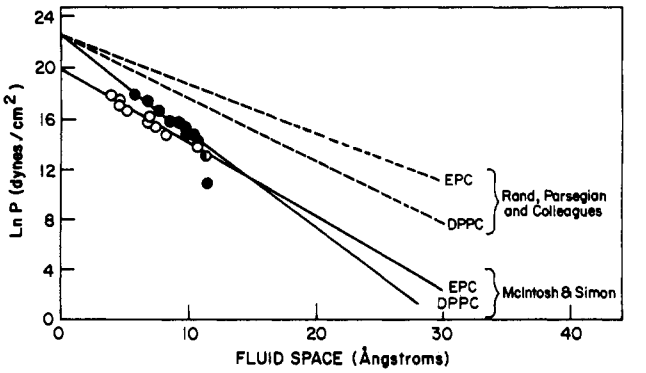

FIGURE 6: Plots of natural logarithm of osmotic pressure, P, vs. fluid spacing, d_f, for DPPC and EPC. The dashed lines for DPPC and EPC are from Lis et al. (1982a). The circles (open for EPC and closed for DPPC) show d_f values calculated from the data in Table I assuming that d_b remains constant. Thus, $d_f = d - d_b$, where d_b = 51.9 Å for DPPC and d_b = 47.8 Å for EPC. The two solid lines are least-squares fits to the respective sets of circles and have osmotic pressure axis intercepts of 4.7×10^9 dyn/cm^2 for DPPC and 4.0×10^8 dyn/cm^2 for EPC. The experimental points deviate from the lines as d_f approaches the equilibrium separation, presumably because the van der Waals attractive force becomes comparable to F_h at these separations (LeNeveu et al., 1977).

(Pashley, 1981a,b; Israelachvili & Pashley, 1982; Parsegian & Rand, 1983; Marra & Israelachvili, 1985). E_c is obtained by integrating the empirical curves in Figure 6 from d_f = infinity to d_f = 0. As first noted by Marcelja and Radic (1976), and apparent from Figure 6, the value of E_c is critically dependent on the definition of d_f. By defining d_f as the partial thickness of the fluid layer (LeNeveu et al., 1977; Parsegian et al., 1979; Lis et al., 1982a), one obtains bilayer contact at the point of complete dehydration of the multilayers (dashed lines, Figure 6). On the other hand, the calculation of d_f from Fourier synthesis analysis, as described above, gives the point of contact as the position where the phospholipid head groups from apposing bilayers physically touch each other (solid lines, Figure 6). Although any definition for d_f = 0 is somewhat arbitrary, we believe that our approach provides a reasonable representation of d_f = 0 for calculations of E_c, because d_f cannot decrease any further under more complete dehydration due to steric hindrance of the lipid head groups. That is, some of the water of hydration is localized in the lipid head-group region (Worcester & Franks, 1976; Büldt et al., 1979), and apposing bilayers can be in contact without the removal of this water. We calculate values of E_c as 80 erg/cm^2 for DPPC and 7 erg/cm^2 for EPC, which imply that bilayers in the gel phase adhere more strongly to each other than do bilayers in the liquid-crystalline phase, a result in agreement with the measurements of Marra and Israelachvili (1985). These values for E_c are smaller than those calculated by Parsegian and Rand (1983), due primarily to the difference in definition of d_f = 0 and differences in the value of the decay constant, λ.

Discussion

Both our sampling theorem and electron density profile analysis indicate that for DPPC, EPC, and BPE the bilayer thickness remains constant (with experimental uncertainty of about 1 Å for DPPC and BPE and about 2 Å for EPC) as the bilayers move from their equilibrium separation to within 2–4 Å of each other. This result is consistent with the recent work of Marra and Israelachvili (1985), who found that the thickness of EPC bilayers, as calculated by refractive index measurements, remains nearly constant as the distance between bilayers is changed. Our result is also in agreement with several previous X-ray diffraction studies which used Fourier

analysis as well as calculations of partial lipid thickness based on measured values of ϕ_L. Using the Fourier synthesis approach, Levine (1970) and Janiak et al. (1979) found that the bilayer thickness of gel-state DPPC and dimyristoylphosphatidylcholine (DMPC), respectively, remains constant over a similar range of d as displayed in Figure 1A. White and King (1985) have used the Fourier synthesis data of Torbet and Wilkins (1976) to demonstrate that the thickness of EPC bilayers changes less than 2 Å over the range of d given in Table I. Using measured values of ϕ_L, Levine (1970) calculated less than a 1-Å change in partial lipid thickness for DPPC bilayers, and Reiss-Husson (1967) calculated that the partial lipid thickness of EPC bilayers changes about 2 Å over the range of d given in Table I. Our own gravimetric measurements with EPC (data not shown) are in agreement with those of Reiss-Husson (1967). In contrast, using measured values of ϕ_L, LeNeveu et al. (1977), Parsegian et al. (1979), and Small (1967) calculated approximately a 6-Å change in the partial lipid thickness of EPC bilayers, and Lis et al. (1982a) calculated a 6-Å change in the partial lipid thickness of DPPC bilayers for this range of repeat period.

There are at least four possible reasons for the observed differences between our results and those of Rand, Parsegian, and colleagues: (1) the limited resolution in the electron density profiles; (2) the partial specific volumes of water and/or lipid being different than 1.0 at low hydration, as argued by White and King (1985); (3) differences in composition of EPC (e.g., chain length and degree of chain saturation); and (4) inaccuracy in the measurement of ϕ_L. All four of these explanations might be contributing factors. However, on the basis of comparisons presented in the previous paragraph and our model calculations (Figure 5A,B) which show that changes in bilayer thickness as large as 6 Å would easily be detected by both the sampling theorem and electron density profile analysis, it seems reasonable to conclude that the largest source of the discrepancy is inaccuracy in the measurement of ϕ_L. The lack of observable change in the wide-angle pattern of the gel state also is strong evidence, at least in the case of DPPC, that the bilayer thickness does not change significantly for the range of d considered in this paper. We note that the Fourier method does indicate that there are bilayer structural changes when additional water is removed from the bilayer by incubating specimens in low-humidity atmospheres (Levine, 1970; Torbet & Wilkins, 1976; McIntosh, 1978). That is, although our analysis shows that d_b remains nearly constant as water is removed from between adjacent bilayers, these previous studies (Levine, 1970; Torbet & Wilkins, 1976; McIntosh, 1978) show that the bilayer thickness and area per lipid molecule do change when additional water, located within the head-group region of the bilayer, is removed.

To quantitate d_f and d_b from the electron density profiles, we have used estimates of 5 and 4 Å for the distance between the center and the outer edges of the PC and PE head groups, respectively. It is difficult to define precisely the boundaries of these head groups, due to their contour and motion (Hauser, 1981; Marra & Israelachvili, 1985). Thus, there is some uncertainty in these estimates. Nevertheless, they are completely consistent with previous X-ray and neutron diffraction studies (Lesslauer et al., 1972; Hitchcock et al., 1974; Büldt et al., 1979) and with the parameters used by Marra and Israelachvili (1985). Moreover, these estimates are used only in our calculation of E_c. The results concerning changes in d_b and A_l, and calculations of the decay constant, λ, are independent of these estimates of head-group size.

Assuming the bilayer is volumetrically incompressible (Evans & Simon, 1975; Parsegian et al., 1979), the area per lipid molecule, A_l, is inversely proportional to d_b (Luzzati, 1968). Our data thus indicate that A_l changes less than 2% for DPPC and less than 4% for EPC over the range of repeat periods shown in Figure 1. In contrast, over an equivalent range of repeat periods, Rand and colleagues calculated changes in A_l of about 11% for gel-state DPPC (Lis et al., 1982a,b) and about 15% for EPC (Parsegian et al., 1979). As described above, the wide-angle diffraction provides strong evidence that the area per lipid molecule does not change significantly for DPPC for this range of d.

The Fourier synthesis analysis can resolve a discrepancy in the value of the lipid compressibility modulus, K, as obtained by two different techniques. Since lateral pressure can be calculated from the measured chemical potential (Parsegian et al., 1979), the osmotic stress technique can be used to calculate K, which is the ratio of lateral pressure to relative area change. However, the published values of K obtained by the osmotic stress technique (Parsegian et al., 1979; Lis et al., 1982b) are 25–50 times smaller than the values measured by the aspiration of unilamellar vesicles with a micropipet (Kwok & Evans, 1981; Evans & Kwok, 1982). Our Fourier synthesis data, which give a smaller change in A_l for a given change in osmotic pressure, and therefore a larger compressibility modulus than found by Lis et al. (1982b), are consistent with the values of Kwok and Evans (1981) and Evans and Kwok (1982), who obtained a 2–3% change in A_l for EPC and less than a 0.3% change for gel-state DMPC at a lateral pressure approximately equivalent to the osmotic pressure of 60% PVP. For EPC, the Kwok and Evans (1981) results are consistent with direct measurements of the curvature elastic modulus (Servuss et al., 1976), which is proportional to the compressibility modulus (Evans & Skalak, 1979).

For uncharged bilayers in excess water, in the absence of an applied external force (LeNeveu et al., 1977), there is a balance between the attractive van der Waals force (F_{vdW}) and two repulsive forces, the hydration force (F_h) and the "undulation" force (F_u) (Harbich & Helfrich, 1984; Evans & Parsegian, 1986). Both F_{vdW} and F_u are long range and vary as $(1/d_f)^3$ (LeNeveu et al., 1977; Harbich & Helfrich, 1984). Therefore, when an osmotic force is applied, calculations similar to those of LeNeveu et al. (1977) show that F_{vdW} and F_u are negligible compared to F_h for values of d_f a few angstroms smaller than the equilibrium separation found in excess water. Thus, for values of d_f smaller than the equilibrium separation by more than 2–4 Å, the applied osmotic force is balanced primarily by the hydration force, and the magnitude of F_h can be equated to the applied osmotic pressure multiplied by A_l. Since our results show that A_l is nearly constant for the osmotic pressure range discussed in this paper, the applied osmotic pressure is directly proportional to F_h. As seen in Figure 6, a plot of osmotic pressure vs. d_f produces an exponential decay, as was previously found by LeNeveu et al. (1977), Parsegian et al. (1979), and Lis et al. (1982a). However, the slopes of the solid lines and dashed lines are different. This is due to differences in the values of d_f. Both groups find similar values of d as a function of osmotic pressure. However, since $d_f = d - d_b$, and since we find that d_b remains approximately constant whereas they calculate that d_b decreases about 6 Å in the range of d considered in this paper (LeNeveu et al., 1977; Parsegian et al., 1979; Lis et al., 1982a), the solid and dashed lines in Figure 6 have different slopes. On the basis of our values for the decay constants of

1.4 Å for DPPC and 1.7 Å for EPC, we conclude that the decay constant of F_h for DPPC and EPC bilayers is not necessarily equal to the diameter of a water molecule (about 2.8 Å).

Since our results indicate that A_l remains nearly constant for both DPPC and EPC for the range of d_f considered here, the solid lines in Figure 6, along with calculated values of A_l, can be used to estimate the volume of water removed from between bilayers at a given osmotic pressure. For example, consider EPC for the pressure experiments shown in Figure 6, which cover a range of repeat periods from d = 59.2 Å at 4.29×10^5 dyn/cm^2 to d = 51.7 Å at 5.71×10^7 dyn/cm^2 (Table I). Using our gravimetrically obtained value of A_l = 67 Å^2 (data not shown) and the change in d_f = 7.5 Å, we obtain a change in volume of the fluid layer of 67 Å^2 × 7.5 Å = 503 Å^3 for this pressure range. Assuming that the volume of a water molecule is about 30 Å^3, we calculate that 8.4 water molecules per lipid are removed as the repeat period is reduced from 59.2 to 51.7 Å. In comparison, for EPC for this same change in repeat period, Parsegian et al. (1979) found that 16.1 waters per lipid are removed and the gravimetric data of Reiss-Husson (1967, Figure 4) indicate the removal of about 10.8 waters per lipid.

For BPE, the quantification of F_h is complicated by two factors. First, d_f changes only about 3 Å (that is about the thickness of one water molecule) in going from excess water to 60% PVP solution (Figure 4B). In this range of d_f, F_{vdW} may be appreciable compared to F_h, so that the applied osmotic force cannot be equated with F_h. Second, when adjacent bilayers are separated by fluid spaces which are only one or two water molecules wide, as they are in fully hydrated egg PE (T. J. McIntosh and S. A. Simon, unpublished results), BPE (Figure 4C), and dilauroyl-PE (McIntosh & Simon, 1986), other interactions may be present, such as interbilayer hydrogen bonding and/or attractive interactions between the amine and phosphate groups from apposing bilayers.

Acknowledgments

We thank Dr. Alan Magid for help with osmotic pressure experiments and calculations and for many useful suggestions. We also thank Drs. Peter Rand and Adrian Parsegian for kindly sending us their experimental values of osmotic pressure. We are grateful to Drs. A. Blaurock, E. Evans, N. Franks, S. Gruner, G. King, V. Luzzati, A. Parsegian, P. Rand, G. Shipley, and S. White for helpful comments and discussions.

References

Blaurock, A. E. (1971) *J. Mol. Biol. 56*, 35–52.
Büldt, G., Gally, H. U., Seelig, J., & Zaccai, G. (1979) *J. Mol. Biol. 134*, 673–691.
Cevc, G., & Marsh, D. (1985) *Biophys. J. 47*, 21–32.
Clunie, J. S., Goodman, J. F., & Symons, P. C. (1967) *Nature (London) 216*, 1203–1204.
Derjaguin, B. V., & Chureav, N. V. (1977) *Croat. Chem. Acta 50*, 187–195.
Evans, E. A., & Simon, S. (1975) *Biophys. J. 15*, 850–852.
Evans, E. A., & Skalak, R. (1979) *Mechanics and Themodynamics of Biomembranes*, Part 1, p 292, CRC Press, Boca Raton, FL.
Evans, E. A., & Kwok, R. (1982) *Biochemistry 21*, 4874–4879.
Evans, E. A., & Parsegian, A. (1986) *Proc. Natl. Acad. Sci. U.S.A.* (in press).
Franks, N. P., Melchior, V., Kirshner, D. A., & Caspar, D. L. D. (1982) *J. Mol. Biol. 155*, 133–153.
Gruen, D. W. R., & Marcelja, S. (1983) *J. Chem. Soc., Faraday Trans. 2 79*, 225–242.
Harbich, W., & Helfrich, W. (1984) *Chem. Phys. Lipids 36*, 39–63.
Hauser, H. (1981) *Biochim. Biophys. Acta 646*, 203–210.
Hitchcock, P. B., Mason, R., Thomas, K. M., & Shipley, G. G. (1974) *Proc. Natl. Acad. Sci. U.S.A. 71*, 3036–3040.
Horn, R. G. (1984) *Biochim. Biophys. Acta 778*, 224–228.
Israelachvili, J. N., & Pashley, R. M. (1982) *Nature (London) 300*, 341–343.
Israelachvili, J. N., & Pashley, R. M. (1983) *Nature (London) 306*, 249–250.
Janiak, M. J., Small, D. M., & Shipley, G. G. (1979) *J. Biol. Chem. 254*, 6068–6078.
King, G. I. (1984) in *Neutrons in Biology* (Schoenborn, B. P., Ed.) pp 159–172, Plenum Press, New York.
King, G. I., & Worthington, C. R. (1971) *Phys. Lett. A 35A*, 259.
Kwok, R., & Evans, E. (1981) *Biophys. J. 35*, 637–652.
LeNeveu, D. M., Rand, R. P., & Parsegian, V. A. (1976) *Nature (London) 259*, 601–603.
LeNeveu, D. M., Rand, R. P., Gingell, D., & Parsegian, V. A. (1977) *Biophys. J. 18*, 209–230.
Lesslauer, W., Cain, J. E., & Blasie, J. K. (1972) *Proc. Natl. Acad. Sci. U.S.A. 69*, 1499–1503.
Levine, Y. K. (1970) Ph.D. Thesis, University of London.
Lis, L. J., Lis, W. T., Parsegian, V. A., & Rand, R. P. (1981) *Biochemistry 20*, 1771–1777.
Lis, L. J., McAllister, M., Fuller, N., Rand, R. P., & Parsegian, V. A. (1982a) *Biophys. J. 37*, 657–666.
Lis, L. J., McAllister, M., Fuller, N., Rand, R. P., & Parsegian, V. A. (1982b) *Biophys. J. 37*, 667–672.
Luzzati, V. (1968) in *Biological Membranes* (Chapman, D., Ed.) pp 71–123, Academic Press, New York.
Marcelja, S., & Radic, N. (1976) *Chem. Phys. Lett. 42*, 129–130.
Marra, J., & Israelachvili, J. (1985) *Biochemistry 24*, 4608–4618.
McIntosh, T. J. (1978) *Biochim. Biophys. Acta 513*, 43–58.
McIntosh, T. J. (1980) *Biophys. J. 29*, 237–246.
McIntosh, T. J., & Simon, S. A. (1986) *Biochemistry* (in press).
McIntosh, T. J., McDaniel, R. V., & Simon, S. A. (1983) *Biochim. Biophys. Acta 731*, 109–114.
Melville, J. B., & Matijevic, E. (1976) in *Foam* (Akers, R. J., Ed.) p 216, Academic Press, New York.
Parsegian, V. A., & Rand, R. P. (1983) *Ann. N.Y. Acad. Sci. 416*, 1–9.
Parsegian, V. A., Fuller, N., & Rand, R. P. (1979) *Proc. Natl. Acad. Sci. U.S.A. 76*, 2750–2754.
Pashley, R. M. (1981a) *J. Colloid Interface Sci. 80*, 153–162.
Pashley, R. M. (1981b) *J. Colloid Interface Sci. 83*, 531–546.
Pashley, R. M., & Israelachvili, J. N. (1981) *Colloids Surf. 2*, 169–187.
Rand, R. P. (1981) *Annu. Rev. Biophys. Bioeng. 10*, 237–314.
Rau, D. C., Lee, B., & Parsegian, V. A. (1984) *Proc. Natl. Acad. Sci. U.S.A. 81*, 2621–2625.
Reiss-Husson, F. (1967) *J. Mol. Biol. 25*, 363–382.
Schiby, D., & Ruckenstein, E. (1983) *Chem. Phys. Lett. 95*, 435–438.
Servuss, R. M., Harbich, W., & Helfrich, W. (1976) *Biochim. Biophys. Acta 436*, 900–903.
Shannon, C. E. (1949) *Proc. Inst. Radio Eng. N.Y. 37*, 10–21.
Simon, S. A., McIntosh, T. J., & Latorre, R. (1982) *Science (Washington, D.C.) 216*, 65–67.

Small, D. M. (1967) *J. Lipid Res. 8*, 551-557.
Tardieu, A., Luzzati, V., & Reman, F. C. (1973) *J. Mol. Biol. 75*, 711-733.
Torbet, J., & Wilkins, M. H. F. (1976) *J. Mol. Biol. 62*, 447-458.
van Olphen, H. (1977) *An Introduction to Clay Colloid Chemistry*, 2nd ed., p 216, Wiley-Interscience, New York.
Vink, H. (1971) *Eur. Polym. J. 7*, 1411-1419.
White, S. H., & King, G. I. (1985) *Proc. Natl. Acad. Sci. U.S.A. 82*, 6532-6536.
Worcester, D. L., & Franks, N. P. (1976) *J. Mol. Biol. 100*, 359-378.
Worthington, C. R., King, G. I., & McIntosh, T. J. (1973) *Biophys. J. 13*, 480-494.

Chloroplast Coupling Factor 1: Dependence of Rotational Correlation Time on Polypeptide Composition†

Jeffrey E. Schinkel and Gordon G. Hammes*
Department of Chemistry, Cornell University, Ithaca, New York 14853-1301
Received January 13, 1986; Revised Manuscript Received February 4, 1986

ABSTRACT: Time-resolved fluorescence depolarization measurements were made on chloroplast coupling factor 1 (CF_1) labeled with pyrenylmaleimide. Rotational correlation times were determined for native CF_1, for CF_1 lacking ϵ and/or δ polypeptides, and for activated enzyme. The rotational correlation time measured is characteristic of the rotation of the entire enzyme. Removal of the δ polypeptide resulted in a 25% smaller rotational correlation time, although the δ polypeptide contributes less than 5% of the mass of CF_1. Removal of the ϵ polypeptide was without effect. Simultaneous removal of δ and ϵ polypeptides produced a 30% smaller rotational correlation time. Activation of CF_1 ATPase by incubation with dithiothreitol reduced the rotational correlation time by 15% relative to that of the latent enzyme. The rotational correlation time of CF_1 with δ and ϵ polypeptides removed is essentially that expected for a spherical molecule, whereas the other forms of the enzyme can be approximated as ellipsoids of revolution; the axial ratio of the latent enzyme is estimated from the rotational correlation time and the intrinsic viscosity. These data indicate that the δ polypeptide significantly alters the shape of the enzyme and that a conformational change accompanies dithiothreitol activation of the enzyme.

Chloroplast coupling factor is an integral membrane protein that catalyzes ATP synthesis by use of a transmembrane proton gradient. The extrinsic portion of the enzyme, CF_1,[1] is water-soluble and can be removed by treatment with EDTA (Lien & Racker, 1971). CF_1 is a latent ATPase comprised of five types of polypeptides with a total M_r of 400 000 (Moroney et al., 1983). The polypeptide stoichiometry is probably $\alpha_3\beta_3\gamma\delta\epsilon$ (Moroney et al., 1983).

Nucleotide binding and catalysis by CF_1 involve the α and β polypeptides (Kambouris & Hammes, 1985). The γ polypeptide is involved in regulation of catalysis, and it may be involved in proton translocation (McCarty & Moroney, 1985). Four cysteine residues have been identified on the γ polypeptide (Nalin & McCarty, 1984; Moroney et al., 1984). Two of the four cysteines form a disulfide linkage; reduction of the disulfide converts the latent ATPase to an active state. A change of conformation is associated with activation (Nalin & McCarty, 1984; Schumann et al., 1985). Of the two remaining cysteines, one is accessible under all conditions (dark site), while the other is reactive only under energized conditions with CF_1 bound to the thylakoid membrane (light site). The δ polypeptide is essential to the functional integrity of membrane-bound coupling factor (tight coupling), although it is not required for binding of CF_1 to the membrane (Patrie & McCarty, 1984). The ϵ polypeptide is a potent ATPase inhibitor and is closely associated with the γ polypeptide (Richter et al., 1985). The ϵ polypeptide contains one cysteine residue that can be modified by sulfhydryl reagents.

Detailed information about the structural organization of CF_1 has been obtained by fluorescence resonance energy transfer methods (Cerione & Hammes, 1982; Snyder & Hammes, 1984, 1985; Richter et al., 1985). These data have shown a structural asymmetry that reflects the configuration of the ϵ and γ polypeptides. This paper describes time-resolved fluorescence depolarization measurements that indicate an important contribution of the δ polypeptide to the shape of CF_1. Measurements made with activated enzyme show that reduction of the γ disulfide changes the conformation of the enzyme.

Materials and Methods

Chemicals. ATP (vanadium free) and dithiothreitol were from Sigma Chemical Co. Pyrenylmaleimide was from Molecular Probes, Inc. Hydroxylapatite (fast flow), octyl glucoside, and nonyl glucoside were from Calbiochem-Behring. DE-23 cellulose (advanced fibrous) was from Whatman. All other chemicals were high-quality commercial grades, and all solutions were prepared with deionized water.

CF_1 Preparation. CF_1 was prepared from fresh market spinach as previously described (Lien & Racker, 1971; Binder

† This work was supported by a grant from the National Institutes of Health (GM13292). J.E.S. is a National Institutes of Health Postdoctoral Fellow (GM09354).

[1] Abbreviations: CF_1, chloroplast coupling factor; CF_1-ϵ, chloroplast coupling factor lacking the ϵ polypeptide; CF_1-δ, chloroplast coupling factor lacking the δ polypeptide; CF_1-(δ,ϵ), chloroplast coupling factor lacking the δ and ϵ polypeptides; EDTA, ethylenediaminetetraacetic acid; Tris, tris(hydroxymethyl)aminomethane.

0006-2960/86/0425-4066$01.50/0